Design and construction of custom inductive receive coils for low-field AFP NMR using hyperpolarized xenon

Jared K. Wiebe

Undergraduate Honours Thesis

Advisor: Dr. Chris Bidinosti

University of Winnipeg

Winnipeg, MB Canada

May 4, 2012

Abstract

Using hyperpolarized gas (HPG) offers the possibility of higher polarization and therefore higher resolution in nuclear magnetic resonance (NMR) experiments and applications of NMR. Adiabatic fast passage (AFP) NMR is a particular NMR technique that is commonly used to measure the polarization of HPG's [1][2][3][4]. The technique requires inductive detection of electromagnetic signals with high signal-to-noise ratio (SNR). A set of inductive receive coils were designed, constructed, and tested with a water sample in AFP NMR at the University of Winnipeg. The receiver functioned successfully giving an $SNR = (37.7 \pm 0.3)$ dB once the experiment was optimized. Suggestions are made to improve on the receiver and overall NMR experiment.

Contents

List of Tables

List of Figures

1 Introduction

The Physics department at the University of Winnipeg is seeking to produce hyperpolarized (HP) xenon gas for applications varying from fundamental physics to medical imaging. The xenon will be used for research in low-field magnetic resonance imaging (MRI) techniques and in particle physics measurements. HP gas has a net magnetic moment alignment (from the nuclei's spins) higher than achievable with Boltzmann polarization (the spontaneous alignments of the magnetic moments of nuclei in an applied magnetic field at room temperature). This hyperpolarization is achieved through optical pumping and spin transfer through collisions of atoms. The HP gas will have higher signal strengths when compared to Boltzmann polarization (sometimes called thermal polarization) in nuclear magnetic resonance (NMR) techniques.

An important component of any NMR experiment is the device that receives the signal. For NMR experiments it is common to receive the signal by electromagnetic induction. The receiver consists of one or more coils, with many turns, designed to detect the precessing spins from NMR techniques. The precessing spins can be modelled as rotating dipoles which produce an electromotive force or emf in a loop of wire with a magnitude proportional to the frequency of precession. An emf is a voltage generated by a battery or by a time varying magnetic field which will induce an electric current, according to Faraday's Law (see section 3.1). The purpose of this project was to design and construct a receiver based on the requirements imposed by the laboratory. The most important goal in any receiver design is a high signal-to-noise ratio; a strong signal is no use if the noise is also comparatively strong.

In this thesis, the technique of hyperpolarized gas, NMR, and adiabatic fast passage NMR are first reviewed. With this background, the theory of receiving electromagnetic signals through induction, intrinsic noise, preamplifiers, circuits, and the signal-to-noise ratio will be discussed. Design considerations for the custom receiver coil given the constraints of the experimental setup at the University of Winnipeg will then be discussed. The performance results of the receiver that was constructed are then discussed including: basic properties and adiabatic fast passage NMR with a water sample using the receiver. Finally, suggestions will be made to improve the experimental setup.

2 Background

2.1 Motivation

The hyperpolarized xenon laboratory will be used for two immediate goals: i) to research low-field MRI using the xenon as the source of the signal and ii) to use the hyperpolarized gas as a co-magnetometer to study fundamental properties of the neutron at TRIUMF. There are some notable benefits of using HPG in MRI and NMR experiments.

Low-field MRI is the same as normal MRI except lower magnetic field strengths are used in achieving the same image resolution. A low-field MRI system means that a conventional magnet can be used instead of a costly superconducting magnet. Also, superconducting magnets are generally immobile compared to conventional magnets.

For MRI purposes using a smaller B_0 (the strength of the main DC magnetic field that gives rise to a net magnetization in a sample/patient) will lower the specific absorption rate (SAR) of electromagnetic radiation since $SAR \propto R \propto \omega^2$ for a weak conductor such as a human, where R is the resistance of the weak conductor and ω is the angular frequency of the signal [1]. The SAR is a measure of the rate at which energy from a radio frequency (RF) electromagnetic field is absorbed by the body. Since $\omega \propto B_0$ then SAR will be lower with lower B_0. Typical acceptable human limits for SAR are 4 W/kg [1]. This therefore enables fast repetition pulse techniques to be used that would be unsafe with higher field strengths because the SAR would be above the human limit.

Using HPG in low-field MRI will lower the susceptibility gradients caused by changing mediums in organic tissue. A gradient in a magnetic field is a change in the local field strength with respect to position, such as $\partial B/\partial x$; a quantity that tells you how fast the magnetic field is changing in the x direction. Different tissues will different magnetic susceptibilities which will give rise to gradients in the magnetic field when one is applied. These gradients are proportional to B_0 and can therefore be reduced by decreasing B_0 [1,11]. Lowering the susceptibility gradient is important when imaging lungs. The medium transitions between air spaces, blood vessels, and lung tissue produce very strong gradients which give rise to a distortion in the image [1].

Low-field techniques also have applications in NMR spectroscopy. The width in a frequency peak will be $\Delta f = \Delta f_N + (\Delta B_0/B_0)(\gamma/2\pi)B_0$, where Δf_N is the natural peak width of the sample, $\Delta B_0/B_0$ is the inhomogeneity of the magnetic field, and γ is the gyromagnetic ratio characteristic to the sample [4]. If the field strength B_0 is lowered, the magnet's homogeneity requirements can be reduced. For example, if one wants to achieve a line width of 1 Hz with a 20 T magnet they would need the field homogeneity to be one part in 10^9. The same line width in Earth's field, 50 μT, only one part in 2000 is needed [4].

In fundamental physics research, the hyperpolarized xenon will be used as a co-magnetometer in the search for a permanent neutron Electric Dipole Moment (nEDM). The discovery of an nEDM would imply a source of violation of time-reversal (T) symmetry. Assuming CPT symmetry (charge-conjugation, parity symmetry, and time-reversal symmetry all together), this would also imply a source of CP-violation (charge-conjugation and parity symmetry). This could help explain some question in physics today as well as open the door to a physics beyond the standard model. In particular the question of the anti-matter/matter asymmetry in the universe [16].

2.2 Hyperpolarized xenon and optical pumping

Hyperpolarization of a gas is the state where a fraction of the spins of the nuclei in the gas are aligned in a particular direction (defined by an external magnetic field) which is higher than what is achievable using Boltzmann polarization. Hyperpolarization of Xe atomic nuclei is achieved using a technique known as spin-exchange optical pumping.

Optical pumping is a technique to polarize atoms beyond what is possible with Boltzmann polarization. The technique exploits several fundamental properties of particles and atoms. The atom has a quantized atomic structure. Electrons have to be in discrete energy levels most of which are degenerate. The electrons in an atom have spin $\boldsymbol{S}$ and orbital angular momentum $\boldsymbol{L}$ quantum numbers. Combining the spin and orbital angular momentum we get the total angular quantum number $\boldsymbol{J} = \boldsymbol{L} + \boldsymbol{S}$. The total momentum of the atom will be $\boldsymbol{F} = \boldsymbol{J} + \boldsymbol{I}$ where $\boldsymbol{I}$ is the nuclear spin. Terms of the atomic Hamiltonian relating to these quantum numbers provide a small correction to the energy levels and sometimes break the degeneracy of energy levels. This is known as the hyper-fine structure once the nuclear spin corrections are taken into account [10].

When an external magnetic field is applied to the atom further splitting occurs. For weak magnetic fields the splitting is proportional to m_F, which is related to the z-component of the total angular momentum of the atom (known as a magnetic quantum number). This is known as the weak-field Zeeman effect (see Figure 1).

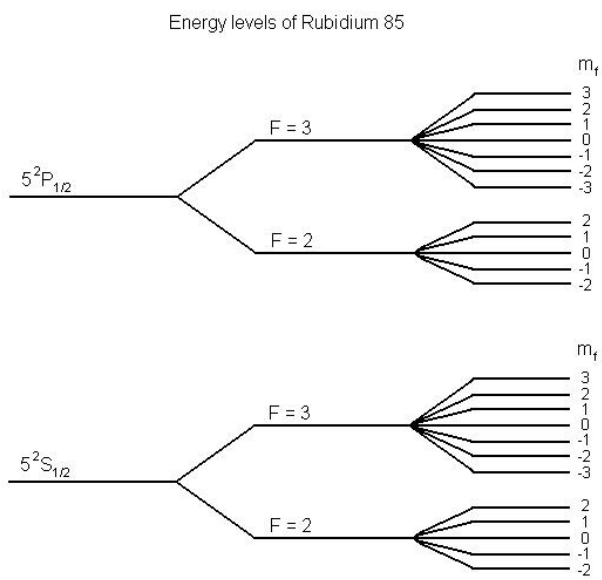

Figure 1 – A diagram showing the weak-field Zeeman effect for Rubidium-85 is shown above as an example. The external magnetic field is weak compared to the field strengths inside the atom. It splits the hyperfine orientation numbers into different energies. The optically pumped atoms will end up all in a particular orientation number. This will cause a net alignment in a particular direction.

The goal of optical pumping is to place the atoms in a state of largest possible m_F. If circular polarized light of correct energy is incident on a atom, while in the presence of a weak magnetic field, the atom will absorb the light, and be excited to a higher energy level. Photons are bosons with spin equal to 1 and m_s is equal to ±1 or 0. Circular polarized light contains photons with $m_s = \pm1$ only (all plus or all minus). If the electron absorbs the photon it must also absorb its angular momentum. The electron now transitions into a higher energy level with but only transitions of $\Delta m_F = 1$ (where Δ indicates the change of) are allowed if the photons are all in $m_s = 1$ (for the sake of argument). The electron spontaneously emits the photon and transitions back down to the original energy level but with the possibility of Δm_F being 0 or ±1. Given some time, statistically the absorption and emission will place the atoms in the same m_F leaving now room for another absorption/emission because there is no $\Delta m_F = 1$ in the higher energy level that exists.

For polarizing xenon one would first optically pump another gas (such as rubidium). Then this gas which has particular m_F collides with the xenon atoms. Since xenon has no valence electrons, the Rb atoms interact with the nucleus of the Xe atom. The Xe atom has spin half. Through spin exchange collisions the angular momentum of the optically pumped Rb gets transferred to the nucleus of the Xe atom. Eventually the majority of the Xe gas will have the same m_F, resulting in a hyperpolarization in the presence of a magnetic field. The details of optical pumping and the spin transfer collision can be found in references [11-13]. It is impractical to optically pump xenon directly. Since the interaction is with the nucleus of the xenon and not electrons, one would need energies on the order of x-rays or gamma-rays to meet the energy requirements to place the nucleus in an excited state.

2.3 Nuclear magnetic resonance

2.3.1 NMR basics

Nuclear magnetic resonance is a phenomenon where nuclei with net spin absorb and re-emit electromagnetic radiation at a particular resonant frequency. Every particle with a net spin has an associated magnetic moment

$$\boldsymbol{\mu} = \gamma \boldsymbol{S}, \tag{1}$$

where gamma is the gyromagnetic ratio characteristic to the nuclei (or particle) in question and $\boldsymbol{S}$ is the spin angular momentum. The z component of the magnetic moment for a nuclei with net spin is

$$\mu_z = \gamma S_z = \gamma m_s \hbar, \tag{2}$$

where m_s is the magnetic quantum number and $\hbar = 1.05 \times 10^{-34}$ J·s is Planck's constant divided by 2π. For a spin-1/2 particle or nuclei $m_s = \pm 1/2$.

For a uniform magnetic field in the z direction, that is for $\boldsymbol{B} = B_0 \hat{z}$, the magnetic moments of the nuclei will align with the magnetic field. The nuclei align in parallel or anti-parallel in the direction of B_0. This is described by the Hamiltonian for such a system:

$$H = -\boldsymbol{\mu} \cdot \boldsymbol{B} = -\gamma S_z B_0. \tag{3}$$

The energy for the system will be

$$E = \pm \gamma \frac{\hbar}{2} B_0 = \pm \mu B_0. \tag{4}$$

For many nuclei grouped together, despite a cancellation of the magnetic moments due to the opposite alignments, there will be a net alignment parallel with the magnetic field. The act of aligning the moments with the field to have a net polarization is Boltzmann polarization. With HPG this external magnetic field still needs to be applied to define an axis for the Zeeman splitting.

After the nuclei are aligned in the magnetic field, electromagnetic radiation is sent into the sample at a resonant frequency known the Larmor frequency given by:

$$\omega = \gamma B. \tag{5}$$

The B is the external magnetic field applied. This radiation will cause the spins to tip into the horizontal plane (relative to the direction of the magnetic field) and the spins precess about B at the Larmor frequency (re-emitting the radiation back out as the spin relaxes back into alignment). The precessing spins can be received via electromagnetic induction treating the precessing spins as rotating magnetic dipoles.

2.3.2 Adiabatic fast passage

Tests were done using an adiabatic fast passage (AFP) NMR technique. The AFP technique is the standard method for quantifying HPG polarization versus proton/Boltzmann polarization [1-4, 11, 12].

AFP NMR is a particular NMR technique where the strength of the B_0 field is varied, being swept through the resonant frequency (set by the RF pulses or B_1 field being sent in)[11][12]. The condition that is necessary for AFP NMR is

$$\frac{B_1}{T_2} << \dot{B}_0 << \gamma B_1^2, \tag{6}$$

where the dot on the B_0 denotes a time derivative. The γ is the usual gyromagnetic ratio characteristic of the sample. The T_2 is a time constant associated with the sample known as the spin-spin relaxation time [11,12].

2.4 Magnetization

2.4.1 Magnetization with Boltzmann polarization

Magnetization in general is the spin excess multiplied by the magnetic moment per unit volume. This can be expressed as

$$M = \frac{\mu}{V} N_{excess}, \tag{7}$$

where $\mu = \mu_z$ is the magnetic moment from the NMR discussion in section 2.3.1, V is the volume of the sample, and $N_{excess} \equiv |N_+ - N_-|$. This is assuming there are N_+ aligned parallel and N_- aligned anti-parallel. This can be rewritten by first defining the polarization:

$$P \equiv \frac{|N_+ - N_-|}{N}, \tag{8}$$

where the $N = N_+ + N_-$ is the total number of nuclei not the excess [15]. The magnetization in general can be written as

$$M = \frac{\mu}{V} NP. \tag{9}$$

With Boltzmann polarization, the number of spins parallel and anti-parallel can be determined using statistical mechanics. The parallel aligned nuclei will have an energy of $E_+ = -\mu B_0$ and the anti-parallel nuclei will have an energy of $E_- = \mu B_0$. The subscript of plus/minus is used to denote parallel/anti-parallel respectively. The ratio of populations is given by a Boltzmann factor:

$$\frac{n_+}{n_-} = \exp\left(\frac{2\mu B_0}{k_B T}\right), \tag{10}$$

where $k_B = 1.38 \cdot 10^{-23}$ J/K is Boltzmann's constant and T is the temperature in Kelvin. The polarization is

$$P = \tanh\left(\frac{\mu B_0}{k_B T}\right), \tag{11}$$

and the magnetization of the sample

$$M = N\frac{\mu_z}{V} \tanh\left(\frac{\mu B_0}{k_B T}\right). \tag{12}$$

In the limit of low field strengths (ie. small B_0) the hyperbolic function can be reduced. The hyperbolic tangent can be expanded in a Taylor series:

$$\tanh(x) = x - .... \tag{13}$$

Therefore for low-field strengths the magnetization is:

$$M = N\frac{\mu}{V}\frac{\mu B_0}{k_B T}. \tag{14}$$

For a water sample, which will be used to first test can calibrate the coil and NMR system, it will have a spin-1/2 from the protons in the hydrogen atoms in the water molecule. The magnetic moment is $\mu = 1/2\gamma\hbar$ for protons, where γ is the gyromagnetic ratio for protons. The spin density of water is

$$\frac{N}{V} = \rho_{w,s} = 2\frac{\rho}{M_w}N_A, \tag{15}$$

where $\rho = 10^6$ g/m^3 is the density of water, $M_w = 18.015$ g/mol is the molar mass of water and N_A is Avogadro's number. The spin density works out to be $6.69 \cdot 10^{28}$ m^{-3}. The total magnetization at small field strengths for water is then

$$M = \left(\frac{N}{V}\right)\left(\frac{\gamma\hbar}{2k_B T}\right)\left(\frac{\gamma\hbar B_0}{2}\right), \tag{16}$$

where the magnetic moment for protons spins is subbed in and the N factor for the total amount of particles with spin in the system. Note that the γB_0 term is the Larmor frequency $\omega = 2\pi f$. Putting in the spin density and the Larmor frequency the magnetization for water is

$$M = \frac{\rho_{w,s}\gamma\hbar^2\pi f_0}{2k_B T}, \tag{17}$$

where f_0 will be called the operating frequency, the resonant frequency of the RF corresponding to the field strength of B_0 (and also the frequency of the signal begin received). For an operating frequency of 25 kHz, the magnetization will be $M \approx 1.9 \times 10^{-6}$ A/m for water in a weak magnetic field.

2.4.2 Magnetization with hyperpolarization

For HPG the polarization factor P is no longer related to the temperature as before. The magnetization is just

$$M = \frac{\mu}{V} NP = \rho_{spin} \mu P, \tag{18}$$

where the ρ_{spin} is the spin density of the gas mixture, and P is the polarization factor. For Xe-129 it has been shown that 70% polarization is achievable [3]. For a Xe-129 nuclei, the spin is 1/2 and the gyromagnetic ratio $\gamma_{Xe} = 73.997 \cdot 10^6$ rad s^{-1}T^{-1}. The natural abundance of Xe-129 is approximately 26% and the gas mixture contains 1% of xenon by volume. Therefore only 0.26% of the mixture is Xe-129. The spin density for xenon-129 in our experiment will be

$$\rho_{X,s} = \frac{N_A P_G}{RT}(0.0026), \tag{19}$$

where N_A is Avogadro's number and V is the volume of the sample. This equation assumes that the gas can be modelled as an ideal gas. Assuming a pressure $P_G = 1$ atm and a temperature of $T = 300$ K the spin density of xenon-129 is $\rho_{X,s} \approx 6.4 \times 10^{22}$ spins/m^3. Plugging this number in with the polarization of 0.7, the total magnetization will be approximately 1.7×10^{-4} A/m; independent of the frequency and therefore the external magnetic field.

3 Theory of inductive detection

3.1 Faraday's Law

We use Faraday's Law of induction to understand how inductive receivers work. A loop of wire in the presence of a changing magnetic field will have an electric current induced in the wire. The magnetic flux is for one loop of wire is

$$\Phi = \int \boldsymbol{B} \cdot d\boldsymbol{A}, \tag{20}$$

where $\boldsymbol{B}$ is the magnetic field and $d\boldsymbol{A}$ is the element of area of the loop [9]. The electromotive force or emf induced will be

$$\varepsilon = -\frac{d\Phi}{dt}, \tag{21}$$

for a single loop of wire. For N identical loops together, the emf is multiplied by a factor of N. The negative sign is there to let us know that any current that is produced by induction will flow in a direction such that the magnetic field the wire creates from the current acts to oppose the change of magnetic field that is inducing the current. This is known as Lenz's law.

In the case of NMR, the precessing nuclei are akin to rotating magnetic dipoles. This rotation will result in a changing magnetic flux in the loop of wire and therefore induce an emf. The emf will alternate with the same frequency as the rotational frequency of the dipole.

3.2 Signal

There are various factors that contribute to signal and to noise. For the signal there is the inductive detector, Boltzmann polarization, and laser/hyper polarization of gas (HPG). The inductive detectors signal is

$$v_s = -\frac{d\Phi}{dt} \propto \omega, \tag{22}$$

and the change of flux will be

$$\frac{d\Phi}{dt} = N_c A \omega \mu_0 M, \tag{23}$$

where μ_0 is the magnetic permeability of free space, A is the area of the coil where the field is rotating through, N_c is the number of turns in the coil, and ω is the frequency of rotation (the frequency of B_1 being sent in) that satisfies $\omega = \gamma B_0$ to get a signal (the B_0 is being swept through this resonance given by the Larmor frequency). The M is the magnetization worked out previously.

For Boltzmann polarization the M is dependent on the external field B_0 (equation 14). The overall signal will be dependent on the inductive detection and the polarization. This leaves the signal from inductive detection and Boltzmann polarization dependent on B_0^2 or ω^2 in terms of frequency.

For Laser/Hyper Polarization the sample is polarized beforehand and does not require a polarizing field B_0. This implies hyperpolarization is independent of B_0 and therefore independent of ω (equation 18) leaving only the term from the change of flux to contribute to the signal from inductive detection. The signal for HPG and inductive detection is dependent on ω.

3.3 Johnson Noise

The intrinsic noise in any NMR system is due to the coil wire of the inductive detector and any weak conductors, such as a water sample, in the AC field (this is excluding any of the electronic devices after the detection). The coil wire of the inductive detector will have some Johnson Noise. Johnson Noise is the fluctuations of electron density at a finite temperature [5]. The Johnson Noise is

$$v_J = \sqrt{4k_B T \Delta f R(f)}, \tag{24}$$

where Δf is the bandwidth of the detector [5], $R(f)$ is the frequency dependent AC resistance, k_B is Boltzmann's constant, and T is the temperature.

The DC resistance is

$$R_{DC} = \rho \frac{L}{A}, \tag{25}$$

where ρ is the resistivity, L is the length of the wire, and A is the cross-sectional area of the wire. For AC currents running through the wire, the resistance changes. As the frequency increases the current travels along the wire closer to the outer surface and ignores the inner area. Qualitatively it is as if, looking at the cross-sectional area of a circular wire, that the wire is being hollowed out increasingly as the frequency of the AC current increases. A complete formula for the AC resistance is

$$R_{AC} = \frac{r_w R_{DC}}{2\delta} \Re\left[(1+i)\frac{J_0[(1+i)r_w\delta^{-1}]}{J_1[(1+i)r_w\delta^{-1}]}\right], \tag{26}$$

where the R_{DC} is the DC resistance, r_w is the radius of the wire, and i is the imaginary number. The $\Re$ signifies that you to take the real part of the argument. The J_0 and J_1 are Bessel functions of the first kind, and δ is the electromagnetic skin depth. The latter is given by

$$\delta = 2/\sqrt{\mu\sigma\omega}, \tag{27}$$

where σ is the conductivity of the material and μ is the magnetic permeability of the wire. The skin depth is the length scale over which the electric current dies off/decays inside the wire. The AC resistance is the DC resistance multiplied by some other function that will be greater than or equal to one, always causing the resistance to increase. A plot of the AC resistance as a function of frequency is shown in Figure 2.

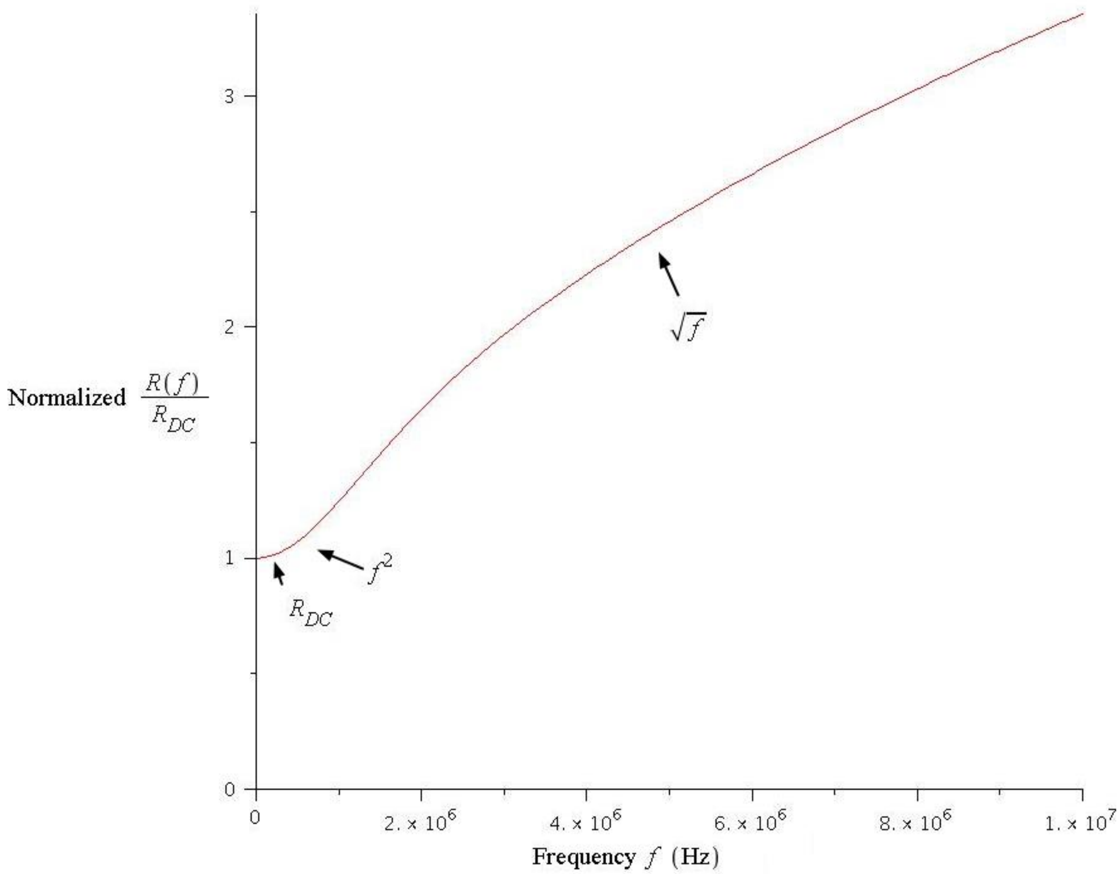

Figure 2 – Plot showing how the resistance depends on frequency for AC circuits (equation 26). The plot is done with the properties of 30 gauge copper wire (which will be used for the coil). Note the operating frequency for our experiment is around 25 kHz which is effectively the DC resistance, shown on the plot. As the frequency increases the dependence of R_{AC} on f changes. Initially it is approx. R_{DC}, then it goes as f^2, and at high frequencies R_{AC} goes as $\sqrt{f}$. The vertical axis is the AC resistance normalized to the DC resistance R_{DC}.

Since the Johnson noise is proportional to $\sqrt{R_{AC}(f)}$ of the coil and the R_{AC} of the wire has three regions shown in Figure 2, then the Johnson noise due to the coil will also have these three regions. For the very low frequency limit we can see the coil resistance is just the R_{DC} and independent of frequency. At low frequencies the AC resistance depends on f^2. At high frequencies the AC resistance of the coil goes as $\sqrt{f}$.

There is also noise due to the NMR sample, such as water, in an AC field. Most samples will behave as a weak conductor in an AC field. This noise can be treated as Johnson noise of a series resistance. Let this resistance be $R_S(f)$ (the subscript S denoting the sample resistance). The resistance of a weak conductor, from a sample in an RF field, is given in reference [11]. This resistance depends on the geometry of the sample and of the RF coil, and their positions relative to one another. The sample resistance R_S is also dependent on f^2.

The total Johnson noise will be the two added in quadrature (assuming the two Johnson noise source are uncorrelated):

$$v_J = \sqrt{v^2{}_{J,S} + v^2{}_{J,C}}, \tag{28}$$

where the subscripts S and C denote sample and coil, respectively.

3.4 LRC circuits

The inductive receiver will be a combination of one or more sets of multiple loops of wire. Looking at the coil we see an LRC circuit, a circuit that contains an inductor L, resistor R, and capacitor C. The induction receiver, no matter what it looks like, will have all these elements. There is resistance due to the wire itself. There is inductance due to the loops of wire. And there will be at least a self-capacitance from the proximity of the adjacent wires in the turns. The emf induced in the circuit can be accounted for by having an AC emf source in the circuit. The signal is sent in to a preamp. The equivalent circuit is shown in Figure 3. The circuit has an ideal voltage source to represent the induced emf in the inductor L. The element A in the diagram is the preamp.

A theory known as Thevenin's theorem is used to analyze circuits [7]. The theorem states that any combination of impedances (R, L, or C), voltage sources, and current sources with two terminals across the circuit can be reduced to a single voltage or current source and a single impedance.

Practically, if one had such a combination of circuit elements and wanted to find the

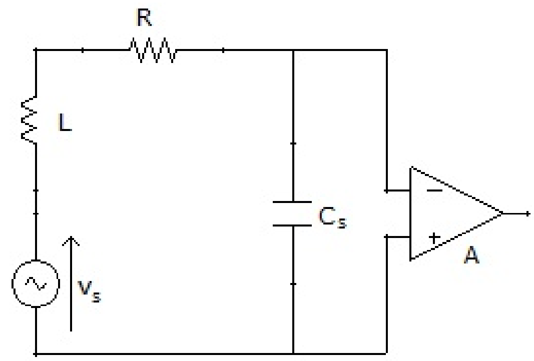

Figure 3 – Circuit diagram for the a single coil. There will be the an inductor and resistance from the wires and then a self capacitance in parallel with the inductor. There is also the AC source v_s in the circuit to represent the induced emf from induction. The signal is sent to preamp A.

Thevenin voltage v_{TH}, they would measure the voltage across the two terminals and that voltage measurement would be v_{TH}. An ideal voltmeter is a resistor across the two terminals $R_{app} \to \infty$ (where R_{app} is an applied resistance). To measure the Thevenin current I_{TH} of this circuit, practically one would measure the current across the two terminals. An ideal ammeter is a resistor $R_{app} \to 0$ across the two terminals. These quantities can be calculated if the circuit elements are known. Figure 4 shows the circuit diagram looking across two terminals A and B.

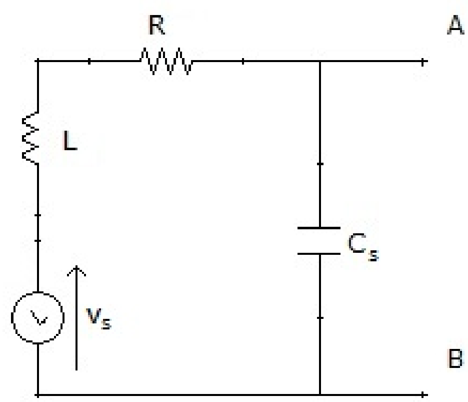

Figure 4 – Circuit diagram of the coil with terminals A and B across the combination of circuit elements. The Thevenin equivalent voltage and current of the circuit are calculated by placing an ideal voltmeter and ammeter across the two terminals, respectively.

The equivalent voltage v_{TH} will be calculated as if there were a resistor across A and B that tends toward infinity. The Thevenin voltage is

$$v_{TH} = v_s \frac{-iX_C}{-iX_C + R + X_L}, \tag{29}$$

where i is the imaginary number, $X_C = 1/\omega C$ is the capacitive reactance, and $X_L = \omega L$ is the inductive reactance. In both reactance's the ω is the frequency of the voltage/current in the circuit.

Using some arbitrary values for equation 29, the equivalent voltage is plotted in Figure 5 to show the behaviour of the voltage. The peak

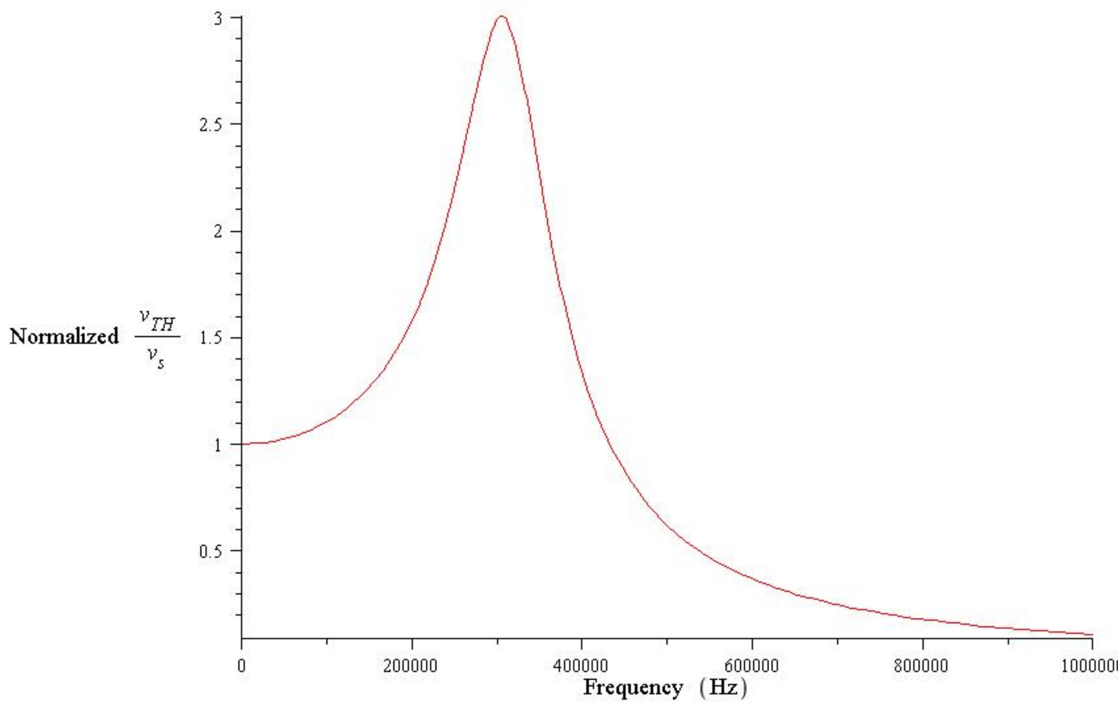

Figure 5 – Equation 29 plotted with some arbitrary values. The equivalent voltage is normalized to the source voltage; this normalized function will be treated as a gain multiplying thee source voltage to get the equivalent. The resonant frequency can be seen on the plot; it is the frequency where the highest gain occurs (the peak).

To find I_{TH}, a resistor is placed across the terminals A and B with zero resistance, creating a short. The Thevenin current is

$$I_{TH} = \frac{v_s}{R + iX_L}, \tag{30}$$

where the R is the resistance from the wire in circuit (treated as resistor in the circuit). An equivalent impedance can be determined using Thevenin's voltage and current by Ohm's Law:

$$Z_{TH} = \frac{v_{TH}}{I_{TH}} = \frac{-iX_C(R + iX_L)}{R + iX_L - iX_C}. \tag{31}$$

The resonant frequency of a circuit is defined as the frequency at which the impedance becomes purely real. The equivalent impedance Z_{TH} found before can be rearranged to

$$Z_{TH} = \frac{R + i\left(X_L - \frac{R^2}{X_C} - \frac{X_L^2}{X_C}\right)}{1 - \frac{2X_L}{X_C} + \frac{X_L^2}{X_C^2} - \frac{R^2}{X_C^2}}. \tag{32}$$

Solving for the imaginary term to be zero, the resonant angular frequency of the circuit is

$$\omega_{circuit} = \sqrt{\frac{1}{LC} - \frac{R^2}{L^2}}. \tag{33}$$

In the limit of a small R the above resonant frequency can be approximated as

$$\omega_{circuit} \approx \frac{1}{\sqrt{LC}}. \tag{34}$$

The resonant frequency of the circuit should be matched to that of the operating frequency of the NMR experiment. To do this a capacitor will be placed across the coil that will change the resonant frequency of the coil according to equation 34. This capacitor will be called the tuning capacitor.

Another quantity used in circuit analysis is the quality factor defined as

$$Q = \frac{\omega_0}{\Delta\omega}, \tag{35}$$

where $\Delta\omega$ is the full-width-at-half-maximum (FWHM) for a given signal at the resonant frequency ω_0. For smaller FWHM, which would give narrower peaks, the Q goes up. The Q is also defined as

$$Q = \frac{1}{R}\sqrt{\frac{L}{C}}. \tag{36}$$

When the circuit is at the resonant frequency, the v_{TH} and Z_{TH} are reduced and can be written in terms of Q. The equivalent voltage becomes

$$v_{TH} = v_s Q, \tag{37}$$

and the equivalent impedance can be written as

$$Z_{TH} = Q^2 R. \tag{38}$$

Note that the circuit is modelling the receive coils. The receive coils will have R_{AC} discussed in section 3.3.

3.5 Intrinsic signal-to-noise ratio

The signal-to-noise ratio (SNR) is the ratio of the signal strength over the noise strength. The signal is the voltage due to electromagnetic induction $v_s Q$ from equation 37. The intrinsic noise of the coil is the intrinsic Johnson noise of the coil and of the sample. The Johnson noise will now have the resistance from equation 38. The intrinsic SNR is then

$$SNR = \frac{Qv_s}{\sqrt{4k_B T \Delta f Q^2 (R_{AC} + R_S)}}. \tag{39}$$

Notice that the intrinsic SNR of the coil does not depend on the Q. Also from previous discussion on noise, we can reduce equation 28 to the resistances added in quadrature. The SNR in general can than be written as

For the SNR there are two regimes to look at; the limit of coil dominated noise (Johnson noise) and the limit of sample dominated noise (noise of weak conductor) [2][14].

For a signal using Boltzmann polarization and inductive receive coils the coil dominated

SNR has three regions of frequency due to the AC resistance of the coil: very low, low, and high. The sample dominated noise does not have this dependence on frequency; the AC resistance has the same form over all frequencies.

The HPG will have the same dependencies on frequency when it comes to noise, but the signal is linearly dependent on ω (rather than ω^2 like Boltzmann polarization). This is due to the magnetization being independent of B_0 field (and therefore ω as well due to the Larmor relation; see equation 18 and section 2.4.2). The results of this analysis is summarized in Table 1, showing the three different frequency regimes for coil dominated noise and the sample dominated noise, the resistance in each case and the SNR for each type of polarization. Table 1 also shows these parameters for using SQUID (Superconducting Quantum Interference Device) detection which we hope to use in the future [2]. The SQUID does not detect the change of flux but measures the field directly making it independent of ω and therefore B_0 [2]. Combine SQUID detection with HPG and there is no longer any dependence on B_0. The noise from the SQUID is a constant noise floor [2].

Polarization		Inductive Detection				SQUID
		Coil dominated			Sample dominated	n/a
	f	$0 \rightarrow$ kHz	kHz $\rightarrow 10^4$	$10^4 \rightarrow \infty$	$0 \rightarrow$ MHz	Noise floor
	R	R_{DC}	$\propto f^2$	$\propto f^{1/2}$	$\propto f^2$	of SQUID
Boltz	SNR	ω^2	ω	$\omega^{7/4}$	ω	ω
HPG	SNR	ω	ω^0	$\omega^{3/4}$	ω^0	ω^0

Table 1 – Table showing two types fo detection, inductive and SQUID. Then two regimes of noise; coil dominated and sample dominated for the inductive method. The coil dominated regime as three frequency limits which show the dependency of R for each limit. The sample dominated resistance has one form for all frequencies. For each type of polarization the SNR is given which depends not only on the polarization type, but also the resistance. Some information was gathered from two papers given in the Reference section:[2] and [14]. The SQUID detection has a noise floor not dependent on resistance [2].

One of the benefits of using HPG in the sample dominated noise regime (such as MRI imaging; a human is a weak conductor), is that the SNR is independent of ω and therefore B_0. You no longer get an SNR increase for higher field strengths, meaning low-field strength MRI is possible.

3.6 Preamplifier

Once the signal is picked up by the receiver coils it must head to a preamplifier. The preamp is used to boost the signal strength with the least amount of degradation to the signal to noise ratio (SNR).

Since the preamp's function is to amplify without SNR degradation we pay close attention to another quantity called the Noise Figure (NF) of the preamp. The NF is a measure of degradation of the SNR and therefore can be used to compare preamps performance. The noise figure is

$$NF = 10 \log \left(\frac{SNR_{in}}{SNR_{out}} \right), \tag{40}$$

where the SNR_{in} is the intrinsic SNR (39) of the signal entering the preamp and the SNR_{out} is the SNR of the signal that leaves the preamp. Standard noise temperature is assumed for this definition of the noise figure (standard noise temp. $T_0 = 290K$; approx. room temperature). The SNR_{out} is always going to be the same (ideal preamp) or larger than SNR_{in} therefore the best possible noise figure is 0 dB. The noise figure is a function of both the source or input resistance R_{in} and the frequency of the signal f; $NF = NF(R_{in}, f)$. The NF can be plotted in a contour plot with one axis as frequency (Hz) and the other source resistance (Ω).

We chose a Stanford Research Systems SR552 preamp instead. This required source impedance is approximately 1000 Ω for a frequency of 25 kHz resulting in an $NF = 1$ dB. The noise contours of both the SR560 and SR552 are displayed in Figures 5. The SR560 is included because the noise contour displays the high frequency behaviour and the SR552 was cut too short (both figures are taken from the operations manual provided by Stanford Research Systems [5,17]).

Re-writing the SNR ratio in the NF in terms of gain from the preamp and noise will help in analyzing the NF behaviour. The ratio is

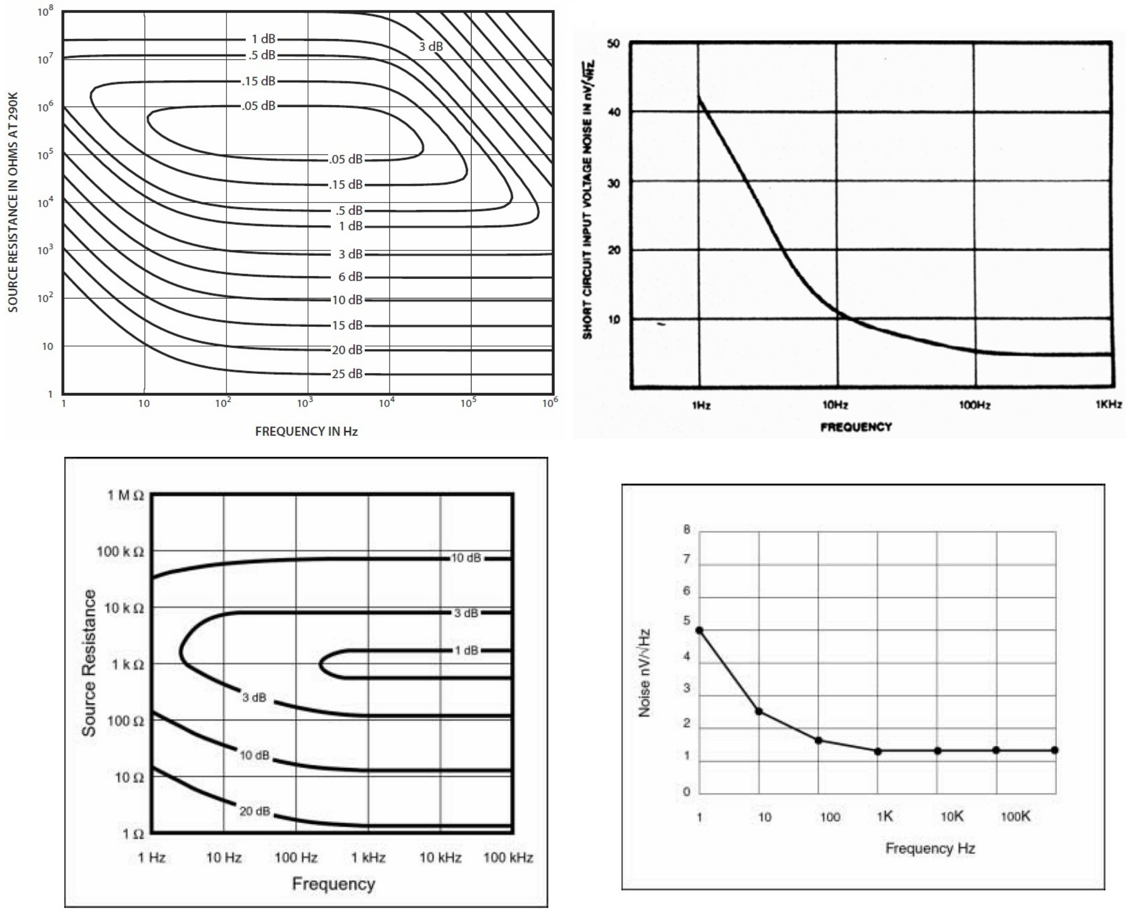

Figure 6 – The noise contour and low frequency behaviour for the SR560 preamp is in the top row. The information about the SR552 is on the bottom. At an operating frequency of 22-25 kHz this corresponds to a impedance of 10^5 to 10^6 Ω when using the SR552. The NF increases for lower frequencies due to 1/f noise shown in the plots on the right. As you lower the resistance, the noise of the preamp starts to dominate. At high frequencies, the starts to get attenuated by the shunting capacitance of the preamp. At high resistances the NF increases due to the current noise of the preamp that is dependent on the source resistance [5,17].

$$\frac{SNR_{in}}{SNR_{out}} = \frac{\sqrt{G^2 n_s^2 + n_{pp}^2}}{G n_s}, \tag{41}$$

where the G is the gain factor of the preamp and is dependent on the source resistance. The n_s is an noise from the source. The n_{pp} is any noise from the preamp, including 1/f noise and current noise (which depends on the source resistance). As the source resistance increases, the all of the terms in equation 41 depend on the resistance and the NF will increase. This behaviour can also be seen in the noise contours. You can see in Figure 6 that as you decrease in source resistance, the noise figure increases. Although the noise of the source is decreasing, and therefore the SNR_{in} is increasing, the noise of the preamp starts to dominate and the NF increases (the amplifiers input voltage stays relatively constant). As the source resistance increases, SNR_{in} will start to decrease, and the Johnson noise of the source resistance starts to dominate and the signal is lost. The current noise of the preamp is IR_{source}; so as the source resistance increases higher the NF will eventually start to increase. Looking at both figures again as the frequency of the signal decreases it starts to get into the $1/f$ noise region. The plots to the right of the contour show the noise of the preamp and it's dependence on the frequency. If the frequency decreases to much $1/f$ starts to dominate. At high frequencies (looking at Figure 6) the NF also starts to increase. The signal starts to get attenuated by the shunting capacitance in the preamp circuit [5, 17].

4 Coil design

High SNR and mechanical stability were two important design features. The number of turns normally is a parameter that is always desirable; it is noteworthy however that the intrinsic SNR is independent of the number of turns in the coil dominated regime. The signal $v_{TH} \propto N_C$ and the resistance of the coil is $\propto N_C^2$. Since the signal is Qv_{TH} and the noise is $\sqrt{4k_BT\Delta VQ^2R_{AC}}$ then we have the $SNR \propto v_{TH}/\sqrt{R_C} \propto N/\sqrt{N^2}$, which is independent of N.

Since the noise from the coil is proportional to the $\sqrt{R_{AC}}$ of the coil you require as small as resistance as possible to reduce the thermal noise of the coil as much as possible (you could also lower the temperature too). The equivalent impedance of the coil is $Z_{TH} = Q^2R_{AC}$ from equation 37. An impedance transformation can be done using Q. Recall that the SNR is independent of Q so raising or lower Q will not change the SNR (equation 39).

Background noise is a major consideration when designing these coils. The reduction of any background fields in your NMR signal can be achieved by reducing the sensitivity of the receiver outside the interest. In this case the sample is the are of interest and will be paced inside the coil. Using the coil design discussed in C.P. Bidinosti, et al. [1] as a starting point for the coil design, a similar coil designed was developed. This coil design from reference [1] is shown in Figure 7. The design implements two side coils, wound opposite relative to the coils on the top and bottom, that have the same flux as the M coils due, from a uniform external magnetic field. When the signal from a uniform external field, due to each coil is added together, the signal will cancel. This design reduces the sensitivity to outside fields.

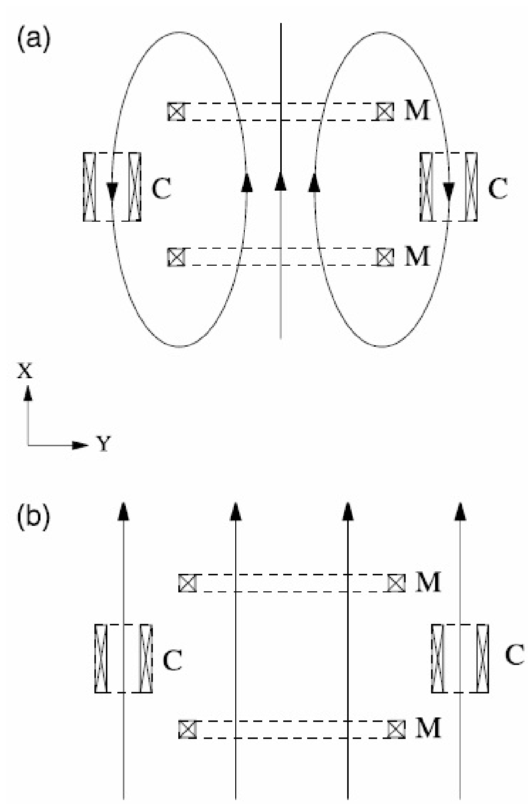

Figure 7 – This coil design is taken from the paper in reference [1]. a) Diagram shows a signal inside the coil assembly. The two coils labelled M will be wound opposite, relative to the two side coils labelled C. The source inside will be added together for all four coils. b) An external uniform field is applied across the coils. Since the coils are wound opposite relative to one another the signal will be subtracted from one another. All coils must have the same magnetic flux from external field (area, number of turns will be the two parameters to adjust).

If the two side coils, C, were stretched around (out of and into the paper) to wrap around the area where the sample is, the same goal would be achieved. Figure 8 shows the top view of the stretched coils. Looking at the currents from the stretched coils, the ends of the C coils, now wrapped around, are right next to one another and the currents travel in opposite directions (the current induced by electromagnetic induction). The same coil designed was achieved by having one side coil, around the sample, on the inside, and on larger coil surrounding the sample.

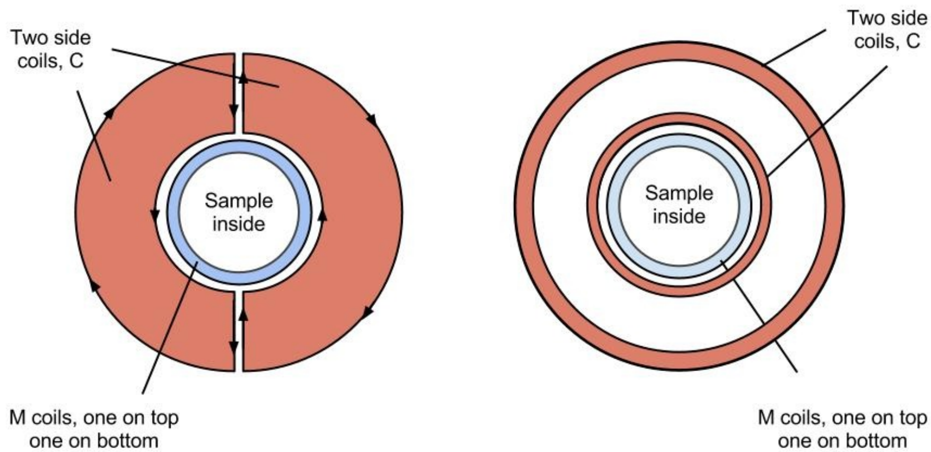

Figure 8 – The diagram on the left shows the top view of the coil design from Figure 7. The C coils are in red and the M coils are in blue, the sample is inside in the middle. The C coils are stretched out and wrapped around and the arrows indicate the direction of a current flow from an induced emf. The straight ends next to one another have a current travelling in opposite directions. An equivalent coil is shown to the right. The ends are merged together and the outside becomes one coil and the inside another.

The design now consists of three inner coils that are adjacent to sample and are wound in the same manner and one outer coil wound opposite relative to the inner coils. The magnetic flux from a uniform external field must be equal in all four coils. To get a receiver with more than four coils, the coil number is increased. The result is an inner solenoidal coil with an outer coil that is larger with less turns. The two coil formers and collars can be seen in Figure 9 and the final coil wired is in Figure 10.

The receiver must fit inside the transverse RF coil. This limits the outer coil to being no larger than 4 inches in diameter. The inner coil is set by the sample size. By convenience a 250 mL bottle was used for the sample size. The inner coil former was chosen to be 2.25 inches. The inner coil and outer coil must have the same flux to an external field. Letting the outer coil have 1/3 the turns of the inner coil sets the radius of the outer coil at $\sqrt{3}r_{inner}$, where r_{inner} is the radius of the inner coil.

To effectively kill off any noise the self resonances of each coil must be higher than the operating frequency. Since the properties of each coil will be different, this could cause uneven gain in the signal received. The self capacitance of each coil should be made as small as possible pushing the self resonances up. To reduce the self capacitances the distance between adjacent windings was increased with coated wire. Figure 5 shows this gain from one coil. There will be two with different resonant frequencies.

The windings on the outer coil were recessed into the coil former to allow the receiver to fit into the RF coil former. This recession on the outer coil caused the inner coil to be recessed slightly to make sure the $\sqrt{3}r_{inner}$ was satisfied. The two coil formers were fastened together with two collars. Two holes were drilled all the way through the outer coil former, collar, and inner coil former to allow a screw to hold all of the pieces together (the screw was also recessed into the outer coil former). This design would allow both coils to stay in place with respect to one another and be modular to allow easy access for maintenance and modifications. The coils are shown in Figures 9 and 10.

5 Experimental setup

Available at the University of Winnipeg, a set of shimming coils were to produce the B_0 field. The experiment was placed in a set of large coils designed to match the Earth's magnetic field in strength but in the opposite direction, eliminating Earth's magnetic field in a direction of choice inside the coils. An existing transverse radio frequency coil was used designed and constructed by a graduated Physics student from the University of Winnipeg, Mike Lang. This RF coil was used as the B_1 coil, tipping the spins away from alignment causing them to precess.

A preamplifier was used to boost the signal before being sent to the lock-in amplifier. Details of the importance of preamp selection was discussed previously. An amplifier was

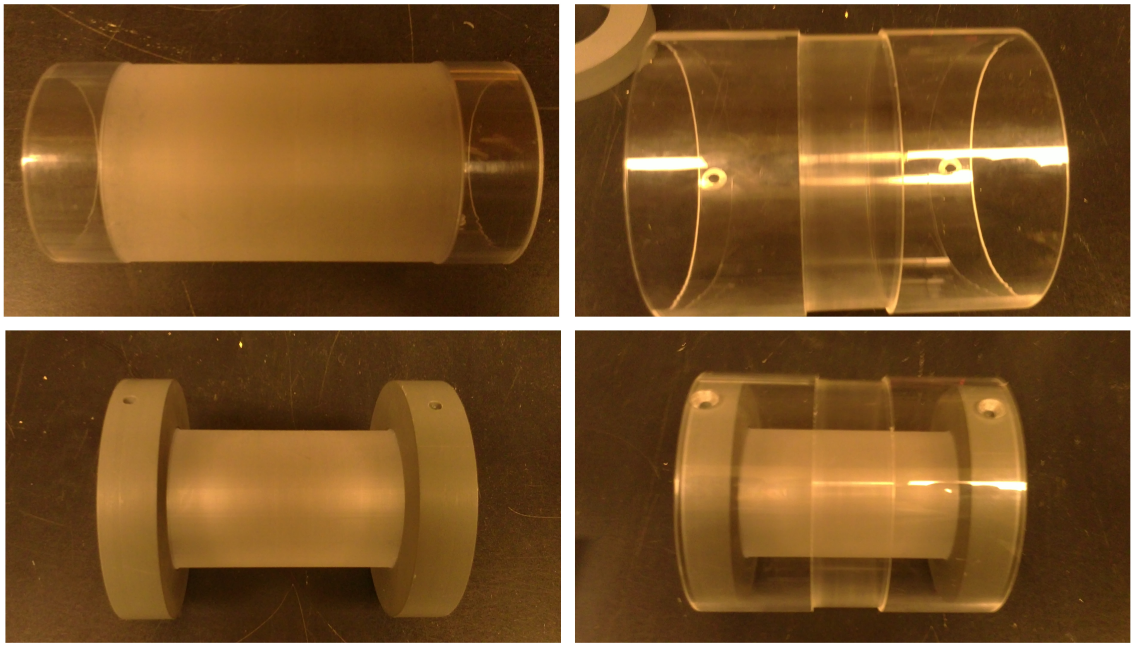

Figure 9 – Top left: the inner coil former. The opaque section in the middle is the recessed area where the inner coil is wound. Top right: the outer coil former; the recession here where the outer coil is wound is more noticeable. Bottom left: the inner coil with the collars on. Bottom right: the full assembly without wires. In all pictures the two holes seen are lined up when assembled to place the plastic screws.

needed to supply 9 to 12 amps to the B_0 coils. The current needs to be swept through the appropriate value that produces the desired B_0 (the one for your resonant frequency) at $\approx$ 500 mHz. To do this a function generator was used to produce a ramp signal (sawtooth curve). Another function generator will be used to drive the B_1 coil and a dummy coil (the purpose of the dummy coil will be explained in section 5.2). A lock-in amplifier was used to acquire the signal from the receiver coil (the sync output from the function generator was used for B_1 and sent as the reference for the lock-in). The receiver signal was then sent out to an oscilloscope along with the ramping current for display. Software for the scope was used to acquire the data and save onto a computer. A block diagram of the setup is shown in Figure 12.

A tuning capacitor is placed across the receiver circuit so that the receiver overall (not the individual coils) has a self resonance the same as the operating frequency of 25 kHz. The first task to set the receiver coil into the RF coil and orient the receiver coil to minimize

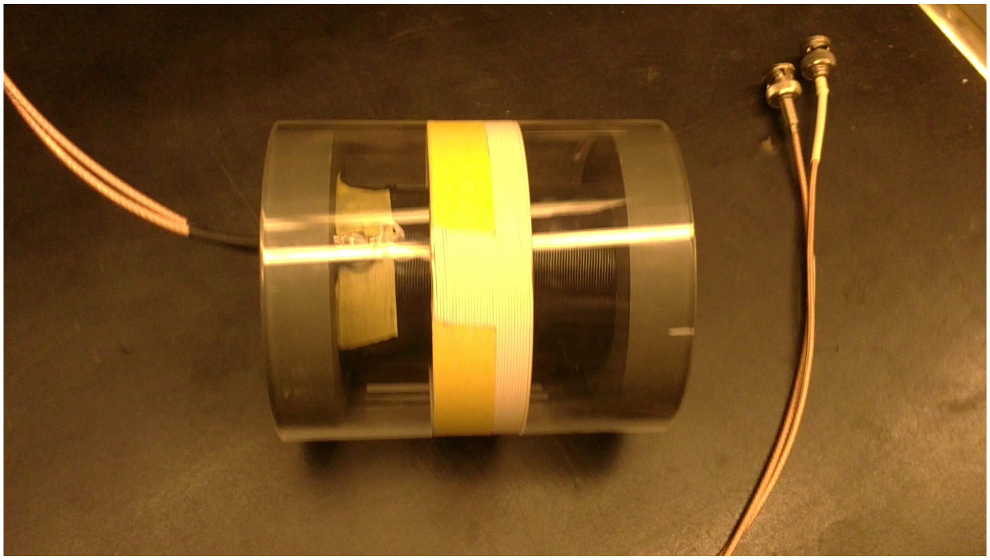

Figure 10 – Picture showing the complete receiver coil. The white wire is the outer coil and the black is the inner coil. They are wired separately to BNC cables so that when the are added together it adds the a signal from inside the coil but subtracts off external sources.

the inductive coupling with the RF coil. This turned out to be very difficult. No particular position in the coil seemed to get rid of the cross talk completely. The cross talk is most likely due to the coupling between the outer receiver coil and the RF coil due to their close proximity.

Next the Receiver and RF together are placed in between the B_0 coils (B_0 coils were not on). It was highly susceptible to rotational position (the RF and receiver are fixed with respect to one another) relative to the B_0 coils. It is possible this is due to coupling between the RF coil and the B_0 coils changing the magnetic field produced by the RF coil. The orientation of the receiver and RF coil are adjusted to achieve the lowest cross-talk.

To reduce the inductive coupling from the RF a dummy coil was used. The dummy coil was placed next to the RF and receiver coil assembly, inside the B_0 coils (the direction of the dummy coil's dipole signal will be parallel with the receiver's cylindrical axis). The dummy coil is set to a field strength such that the signal receive by the receiver is matched in strength to the cross-talk received from the RF. The phase from the dummy coil was set to 180 degrees to that of the phase of the RF cross-talk. When signal from the fields

Figure 11 – Top left: the outer box coils surrounding the equipment inside are designed to eliminate the Earth's magnetic field inside the box. Right in the middle is the transverse RF coil (black former with copper wire on paper surrounding the former). Inside the RF coil(not visible in the picture) is the receiver coil. The two grey coils on either side of the RF and receiver are the B_0 coils. In the lower right side of the picture the blue box is where the tuning capacitor is placed and the grey box is the preamp. Right: Amps used for driving the B_0 coils and the Earth's field compensation coils. Bottom Left: Lock-in amplifier on the bottom and a function generator on top. The lock-in receives the signal from the preamp and send it out to a scope. A function generator is used for controlling the ramp rate of the B_0 field and another to drive the RF and a dummy coil (dummy coil not in picture).

of the dummy coil and RF coil are begin received, the opposite phases should ensure the cancellation of the cross-talk. Ideally this dummy coil should be as close as possible to the outer receiver coil so the field strength required to match the signal from the RF coil is much smaller than the RF field strength (note the difference of field strength and the strength of the received signal). Measurements of the individual field strengths of the RF and dummy coil were taken as close as possible to the position of the sample. The field of the RF was approximately 300 times stronger than the dummy coil field strength. It could be around 1000 times stronger at the sample position. It is safe to say the dummy coil would not interfere with the AFP NMR.

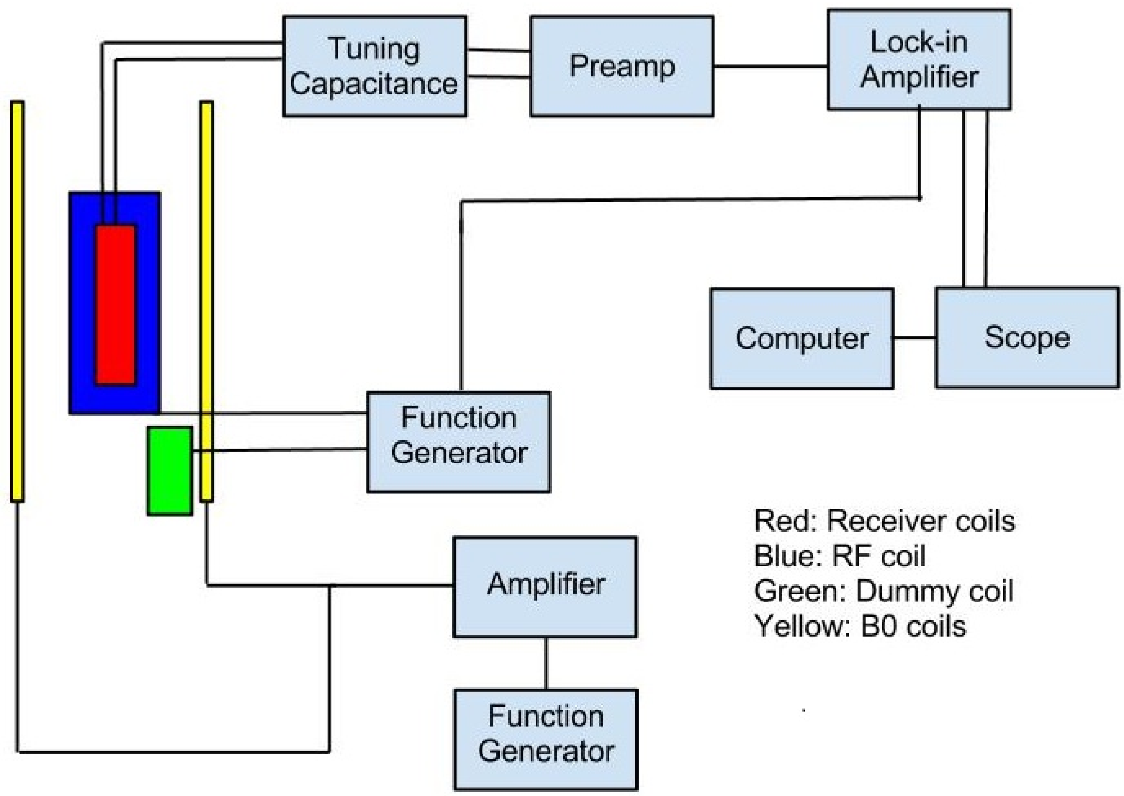

Figure 12 – Block diagram showing the setup of the lab equipment. The two lines from the receive coils to the tuning capacitor are because the coils have separate wires (receive coils shown in Figure 10). The snyc output on the function generator driving the RF coil is sent to the reference on the lock-in and set to the RF channel, not the dummy coil channel. A function generator is sent to the amplifier that drives the B_0 coil to control the ramp rate (a sawtooth curve).

6 Results

6.1 Coil performance

The coil formers were machined by Jarod Matwiy, the machinist at the NRC in Winnipeg. The coil formers and collars can be seen in Figure 9 and Figure 10 shows the full receiver coil wound and wired.

The inner and outer coils were wired separately. The inner coil has 200 turns and the outer 66 turns, satisfying the 1/3 factor that was set in order to have the same flux to an external field. The DC resistance, inductance, self resonances, FWHM of the self resonance, Q and self-capacitances are summarized in Table 2 for each coil. The Q and self-capacitances are calculated quantities from the measure self-resonance and inductance of each coil.

Table 2 – Summary of the number of turns, DC resistance, inductance, self resonance, FWHM at self resonance, Q, and self capacitance of each coil in the receiver. The Q and self capacitance are derived from the other measurements.

Coil	Turns	R_{DC} (Ω)	L (mH)	f_0 (kHz)	$\Delta\omega$ (kHz)	Q	C_s (nF)
Inner	200	12.2(1)	0.115(5)	315	19	16.7	2.2(4)
Outer	66	6.6(1)	0.054(5)	635	34	18.7	1.2(4)

The goal was to increase the self resonances of the coils so that it was not near the operating frequency, reducing the possibility of uneven gain from each coil. Looking at equation 29 and Figure 5 the effective voltage of any signal is proportional to both L and C self of the coils. Plotting the equivalent voltage, i Figure 13, normalized to the source voltage, calling this the Gain, the self resonances of each coil are sufficiently far away from the operating frequency so that the gain from each coil is the same at that frequency.

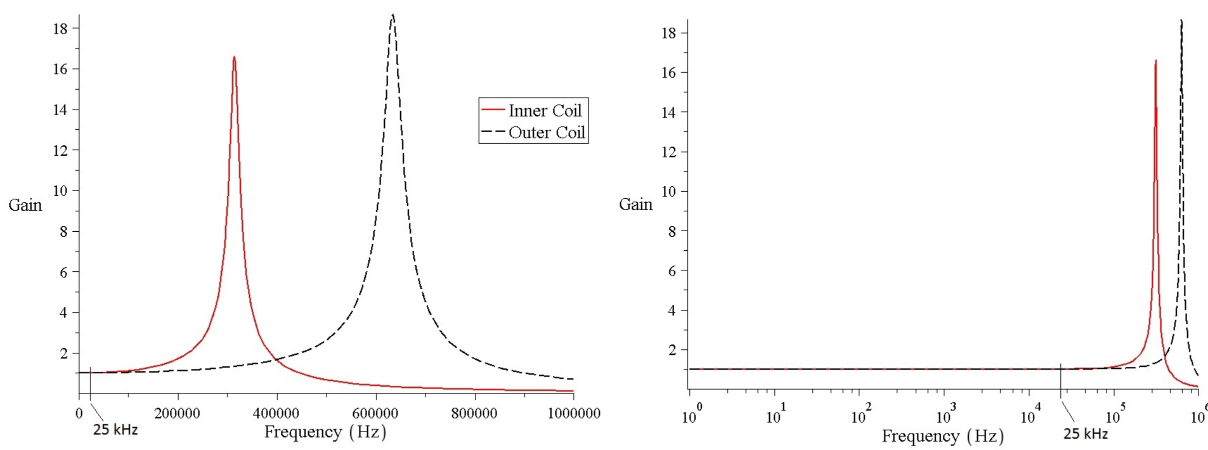

Figure 13 – Plot of the gain from each coil as a function of frequency. The red curve is the inner coil, the dashed, black line the outer coil. The right plot is the same as the left except the frequency is on a log scale. Our operating frequency is approximately 25 kHz. If the operating frequency was higher, for example close to the self resonance of the inner coil, any external field received would not be killed off effectively; even though the coils have the same flux from the field, the gain from one would be higher than the other. As it is at 25 kHz the gain from both coils are the same. The gain is the Q factor multiplying the source voltage.

Another interest was how well the outer and inner coil combinations killed of any external noise source. The coil was tested with an external dipole source (a small coil) at incremental distance away from the receiver both on-axis and perpendicular, at 3 different frequencies (including the operating frequency). Ideally, with just the inner coil the signal should fall of as a dipole r^{-3} and with the outer coil compensation, fall off as r^{-5}. Figures 14 and 15 show the plots of the comparison of the inner coil versus both coils at 25 kHz, on axis and perpendicular to the receiver coil, respectively.

The on-axis measurements were not as expected. The powers were -2.4 and -2.9 for the inner coil and both coils respectively. The addition of the outer coil still made the receiver less sensitive to the external source, but not by the factor we had hoped. The perpendicular measurement is better; -2.2 and -4.3 for inner coil and both coils respectively. This is almost the -3 to -5 change that we were expecting. Since the coil was designed to eliminate any external uniform fields, it's possible that since the dipole is not perfectly uniform at these close distances that the desired effect is not achieved. There could be another reason that is currently unknown.

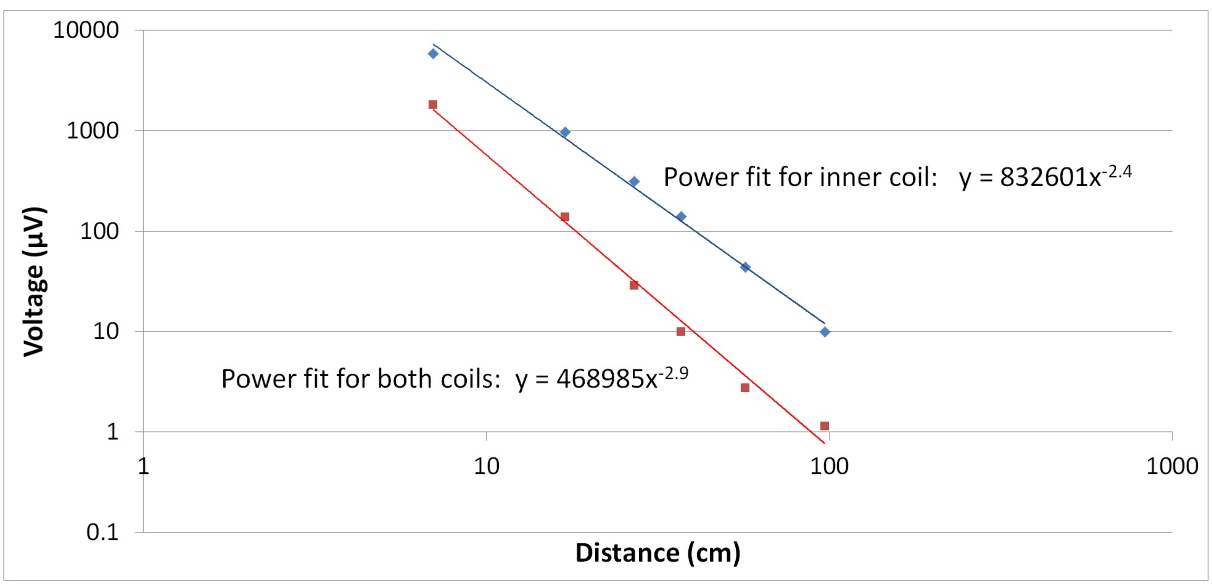

Figure 14 – The blue points are from just the inner coil while the red is inner plus outer. The plot is on a log-log scale. Although the curves do not follow the r^{-3} and r^{-5} as desired, the curve for both coils is steeper implying the external source dies of faster with distance as opposed to the signal from just the inner coil. The inner coil power is approx. -2.4 and both coils is approx. -2.9.

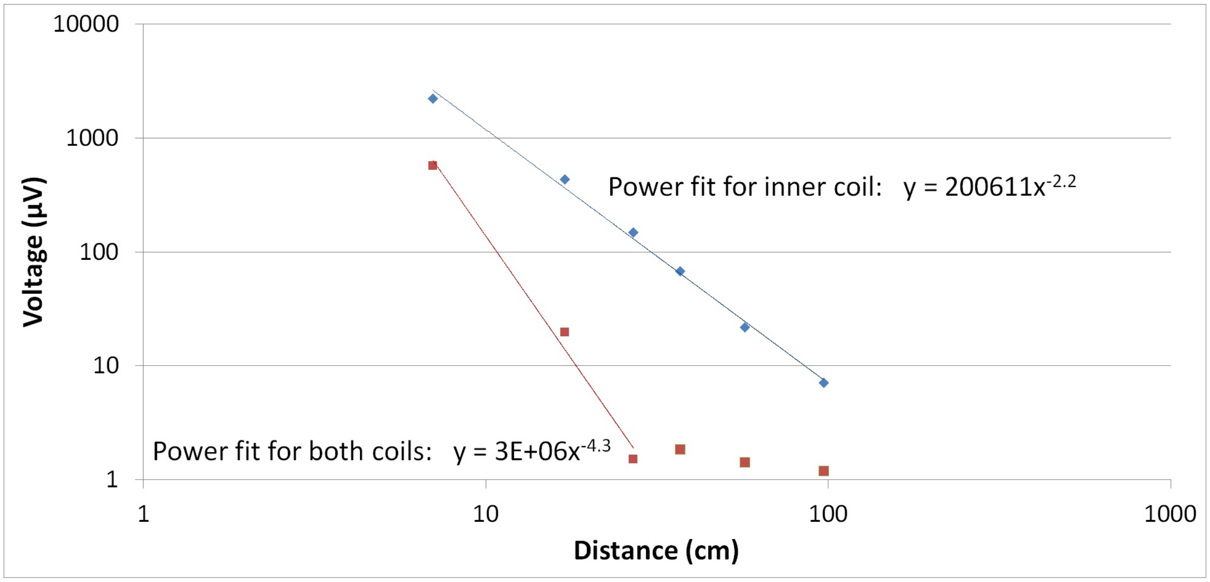

Figure 15 – Same plot as Figure 14 except this one is perpendicular to the receiver coil instead of on axis. The blue data points are for the inner coil only and the red for both coils. The data points of the signal from both coils falls off faster than the on-axis measurements. The inner coil power is approx. -2.2 and both coils is approx. -4.3. The three higher distance points for both coils show behaviour of a noise floor.

6.2 Proof of AFP signal

A water sample was used for the AFP NMR. The dummy coil successfully eliminated the inductive coupling. An AFP signal from the water sample was achievable in a single pass (one sweep through the resonance by the changing B_0). Normally the signal is averaged over 16 to 64 pass through the resonance. Averaging is done nonetheless to improve the data. Figure 16 shows a scope screenshot of 16 averages using the setup described in section 5. The SNR measured for this signal was approximately 28. That is approximately an increase of a factor of 6 in SNR compared to not using the dummy coil setup.

To ensure that the peaks seen are from the protons we can change the offset on the B_0 field. Changing the offset will shift the peaks inward or outward depending on whether the offset is raised or lowered. This is characteristic of the AFP NMR technique and allows us to known the peaks seen are from the spins of the protons and not random spikes in the signal or some other anomaly. This is explained in a diagram in Figure 17. Three screen captures

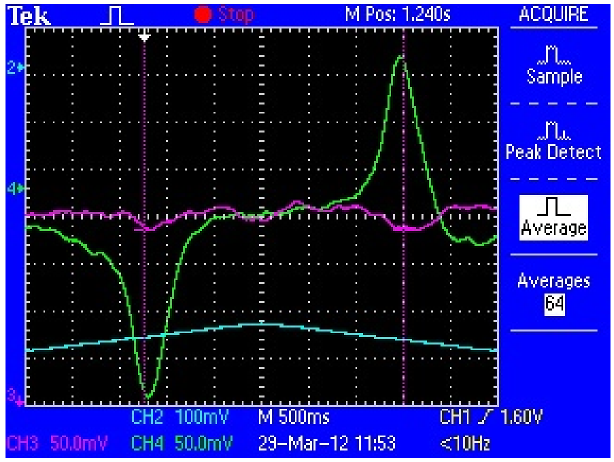

Figure 16 – The proton signal is the green curve, the B_0 is the blue curve. It was a large improvement using the dummy coil. We are able to kill off most of the cross-talk allowing better resolution to be used on the lock-in amplifier.

are shown in Figure 18 that demonstrate the change in the B_0 offset and the shifting of the peaks.

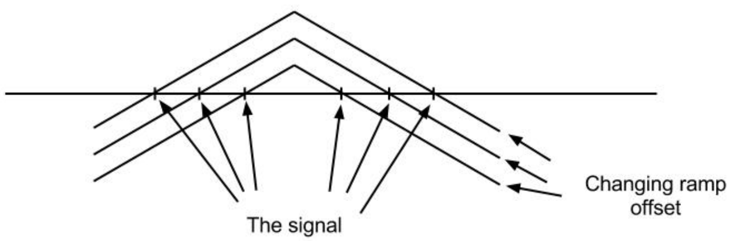

Figure 17 – The changing the offset raises or lowers the overall ramp of the B_0 field. the horizontal line is the signal channel; the intersection (where the peaks appear) is when the B_0 sweeps through resonance. When the offset is changes the intersection occurs at different point, meaning the point where the B_0 field sweeps through is different, and this causes the peaks to shift accordingly. We are not changing any of the B_1 settings.

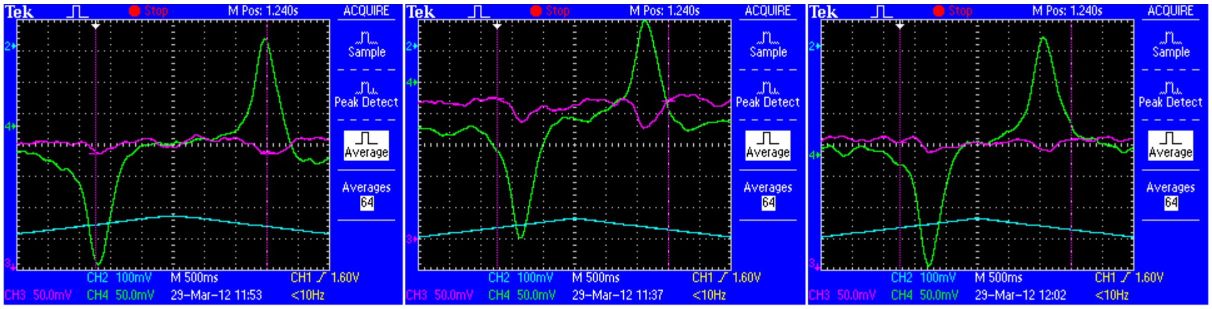

Figure 18 – The signal is the green curve. The B_0 ramp is the blue curve. As the offset is lowered the peaks shift inward. The cursors (the vertical lines) are set in the picture in the left to the peaks; they remained unmoved for the other two pictures. The purple line is just the other channel and is irrelevant.

6.3 Optimization

One parameter to optimize the AFP NMR is the B_1 field strength. While keeping all other parameters constant the B_1 field strength was adjusted at 5 different values. The signals from each B_1 are plotted on the same plot to compare in Figure 19. The goal here is to optimize the AFP NMR experiment as much as possible to get the best signal possible. By adjusting the voltage output driving the B_1 coil, the field strength will change. The B_1 coil functions at approx. 60 μT/A. The best SNR seen was with the voltage driving the B_1 coils set a 1.4 V. This would give a field strength of approx. 8.4 μT. An $SNR = 37.7$ dB was achieved with the 1.4 V setting for B_1.

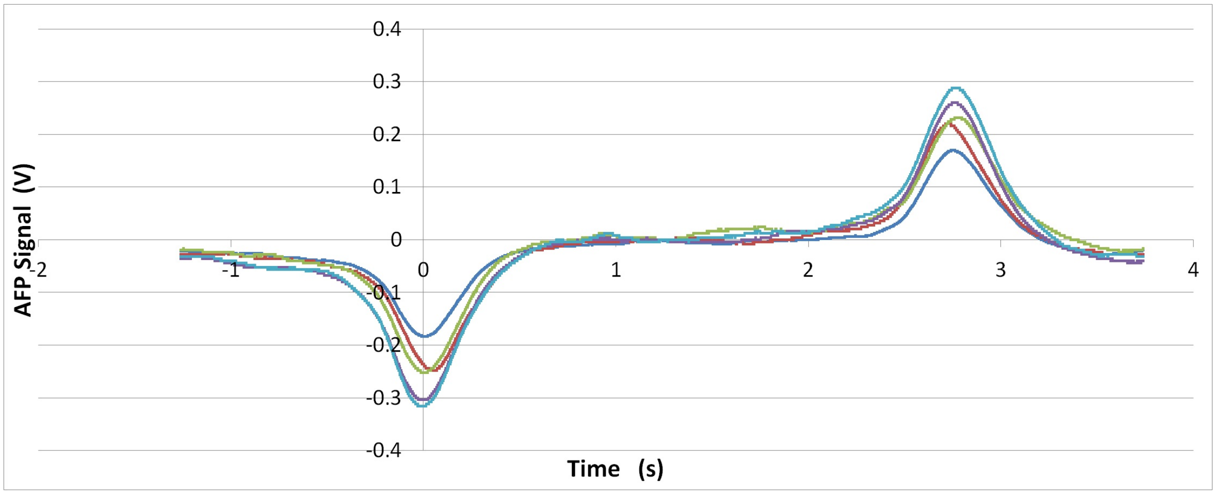

Figure 19 – Plot shows the signal from different B_1 field strengths. You can see the signal strength increases with a higher B_1 field strength. We did a few runs higher than 1.4 V but there was no appreciable gain when compared to the increases in the lower range displayed in the plot. The curve with the strongest signal is the 1.4 V setting. An $SNR = 37.7$ dB was achieved.

The ramp rate was also investigated. The voltage on the function generator that controls the B_0 ramp rate is adjusted by the voltage. The AFP signal with the ramp rate voltage settings of 20, 25, 30, 35, 40 mV are shown on one plot in Figure 20. The best ramp rate setting of those voltage was 30 mV. Higher and lower rates were also measured but a significant decrease in signal strength or an increase in peak width occurred.

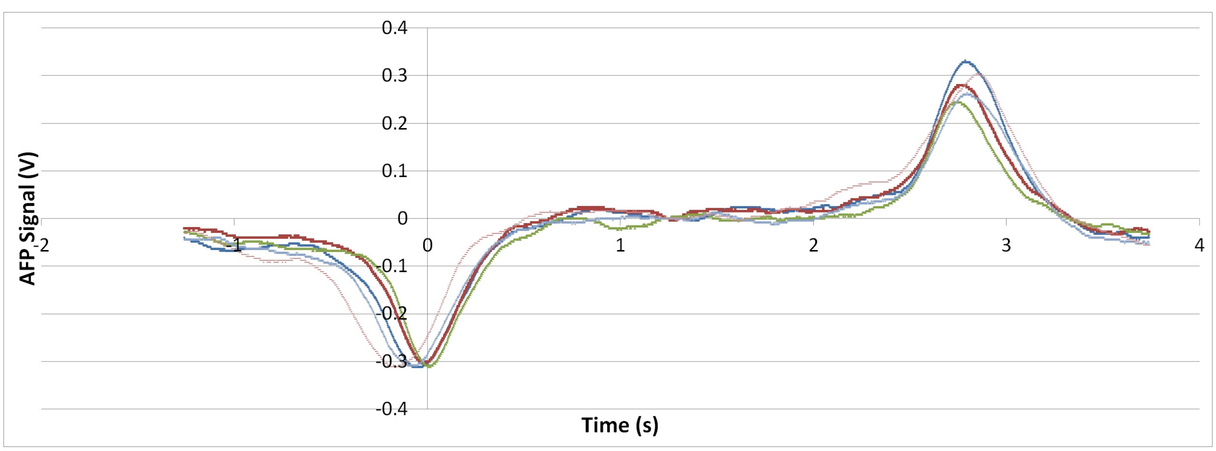

Figure 20 – The plot shows the AFP signal from various ramp rates. The best ramp rate voltage setting was 30 mV on the function generator. From this 30 mV setting, as the rate increased the signal decrease is strength. As the rate decreased the signal decreased in strength and the with of the peak increased.

7 Discussion

Compared to the previous receive coil in place for this experiment the receiver coil that was constructed is an improvement. A simple solenoid was used previously and there were problems with cross-talk that could not be eliminated, but the new receiver coil design is successful in reducing it. The new receiver coil is not the sole factor in reducing the cross-talk; the dummy coil contributed the most. One of the biggest problems with the simple solenoid, and one of the design features in mind for the new receiver coil, was the mechanical stability of the system. With the simple solenoid, physical relaxation was a big setback causing a constant drift when offsetting the signal. The receiver coils are a very tight fit into the RF coil former leaving little room for physical relaxation relative to the RF. Drifting has still occurred on occasion but not consistently, suggesting random vibrations from the environment (building and outside) may be the cause.

The self resonances of each coil were well outside the operating frequency range, provided no uneven gain. The effectiveness of eliminating external noise sources form unknown fields is not as drastic as was hoped for the coil design. Although the receiver coil works well in the AFP NMR, the hope was that more of any external noise would be cancelled out than what was discovered at 25 kHz. Perhaps the non-uniformity of a dipole source caused the results to differ than what was expected

Here are some recommendations for the AFP NMR experimental setup:

i) Replace the current transverse RF coil with a coil that can be farther away from the receiver to reduce the inductive coupling and because the current RF coil has some inhomogeneities due to the non-uniformity in the design. A simple Helmholtz pair would probably suffice. To have this new RF coil inside the B_0 coils this would require the B_0 coils do be moved apart slightly. Changing the current transverse RF might help with physical orientation/mechanical stability. In principle, the receiver coils are orthogonal to the current RF coil (but a signal is still being received) and the receiver is tight fitting in the RF coil former, providing mechanical stability but also leaving little room for adjustment. With a

Helmholtz pair and the receiver coils free, there would be full spatial freedom to adjust the receiver coils relative to the B_1 and B_0. The foundation that the RF and receive coils sit on could also be more level and stable itself.

ii) By moving the B_0 coils farther away to make room for the Helmholtz RF, the increased distance will reduce possible inductive coupling between the B_0 coils and the RF coil and between the B_0 coils and the receiver coils. These changes should reduce the cross-talk overall in the current system. This may introduce inhomogeneities in the field (extra terms in multiple expansion of the magnetic field). If a square Helmholtz coil is used for the RF the B_0 coils would not have to be adjusted as much which might introduce these inhomogeneities.

8 Conclusion and future work

The goal was to design and construct a receiver coil for a hyperpolarized xenon laboratory at the University of Winnipeg. The coil functioned successfully providing very strong signals when compared to the previous results using a different coil. The next step would be to successfully perform the AFP NMR technique with HP xenon gas. This experiment can be used to measure the polarization of the xenon gas (proportional to the signal strength) which will help to optimize the optical pumping/polarizing process to achieve high polarization.

Another system, both pumping/polarizing and AFP NMR, will be setup at the University of Winnipeg. The current one will be used for research in low-field MRI techniques and the other for nEDM experiments. Once the method is well known and high polarization is achieved a replica of the xenon polarization setup will be constructed at TRIUMF where the nEDM experiments will take place [16]. Also, SQUID's (superconducting quantum interference device) detection will be used for the low-field MRI research; inductive receivers will always be limited by the thermal noise of the coil, stated in equation 24 (dependent in the resistance and temperature) [2].

References

[1] C.P. Bidinosti, J. Choukeife, P. Nacher, G. Tastevin,*In vivo NMR of hyperpolarized 3He in the human lung at very low magnetic fields*, (Journal of Magnetic Resonance 162, 2003, 122 - 132).

[2] E. Durand, G. Guillot, L. Darrasse, G. Tastevin, P.J. Nacher, A. Vignaud, D. Vattolo, and J. Bittoun. *CPMG Measurements and Ultrafast Imaging in Human Lungs With Hyperpolarized Helium-3 at Low Field (0.1 T).* Magnetic Resonance in Medicine 47 (2002) 75 - 81.

[3] Boyd M. Goodson.*ADVANCES IN MAGNETIC RESONANCE, Nuclear Magnetic Resonance of Laser-Polarized Noble Gases in Molecules, Materials, and Organisms.* Journal of Magnetic Resonance 155 (2002) 157 - 216.

[4] J. Clarke, M. Hatridge, M. Moble. *SQUID-Detected Magnetic Resonance Imaging in Microtesla Fields.* Annu. Rev. Biomed. Eng. 9 (2007) 389 - 413.

[5] *Operation manual for Stanford Research Systems, MODEL SR560 LOW-NOISE PREAMPLIFIER.* 1999, Stanford Research Systems, Revision 2.8.

[6] C. Bowick, J. Blyler, C. Ajluni. *RF Circuit design.* 2nd ed. 2008, Elsevier Inc. Newnes publications.

[7] A. F. Kip.*Fundamentals of electricity and magnetism.* 2nd ed. University of California, Berkeley. 1962,1969 by McGraw-Hill Inc.

[8] Edward M. Purcell, *Helmholtz coils revisited*, Lyman Laboratory of Physics, Harvard University, Cambridge, Massachusetts 02138, 1988.

[9] David J. Griffiths. *Introduction to Electrodynamics.* 3rd ed. Reed College. Prentice-Hall, Inc. Upper Saddle River, New Jersey. 1999.

[10] David J. Griffiths. *Introduction to Quantum Mechanics.* 2nd ed. Reed College. Prentice-Hall, Inc. Upper Saddle River, New Jersey. 2005.

[11] J. G. Powles. *The Adiabatic Fast Passage Experiment in Magnetic Resonance.* Queen Mary College, London. 1957.

[12] B.F. Melton, V.L. Pollak. *Condition for adiabatic passage in the earth's-field NMR technique.* University of North Carolina at Charlotte, Charlotte, NC. Journal of Magnetic Resonance. 2002. 15-22.

[13] Reuben Benumof. *Optical Pumping Theory and Experiments.* Staten Island Community College, Staten Island, New York. 1963.

[14] J. Parra-Robles, et. al. *Theoretical signal-to-noise ratio and spatial resolution dependence on the magnetic field strength for hyperpolarized noble gas magnetic resonance imaging of human lungs.* Carleton University, Ottawa. 2005.

[15] R. Bowley. *Introductory Statistical Mechanics.* 2nd ed. University of Nottingham, Nottingham. Oxford University Press. 1999

[16] J.W. Martin. *Neutron Electric Dipole Moment Search with a Spallation Ultracold Neutron Source at TRIUMF.* University of Winnipeg. TRIUMF Seminar.

[17] *Operation manual for Stanford Research Systems, SR550/552 Voltage Preamplifier.* 1999, Stanford Research Systems, Revision 2.6.